EAST EUROPEAN JOURNAL OF PHYSICS
East Eur. J. Phys. **3**. 74-80 (2021) DOI:10.26565/2312-4334-2021-3-11

INVESTIGATIONS OF LEAD FREE HALIDES IN SODIUM BASED DOUBLE PEROVSKITES Cs_2NaBiX_6(X=Cl, Br, I): AN AB INTIO STUDY†

Shaily Choudhary[a], Shalini Tomar[a], Depak Kumar[b], Sudesh Kumar[c], Ajay Singh Verma[d,*]

[a]*Department of Physics, Banasthali Vidyapith, Banasthali, Rajasthan 304022, India*
[b]*Department of Chemical Engineering, Banasthali Vidyapith, Banasthali 304022, India*
[c]*Department of Physics, Banasthali Vidyapith, Banasthali, Rajasthan 304022, India*
[d]*Department of Natural and Applied Sciences, Glocal University, Saharanpur 247232, India*
**Corresponding author: ajay_phy@rediffmail.com*
Received April 19, 2021; accepted July 14, 2021

Despites the excellent merits of lead based perovskite optoelectronic devices; their unstable nature and toxicity still present a bottleneck for practical applications. Double perovskite has emerged as a candidate for optoelectronics and photovoltaic application because of its nontoxic behaviour and stability in air. We have presented ab-initio study of Cs_2NaBiX_6(X=Cl, Br, I) lead free halide double perovskites. The calculation is carried out using the FP-LAPW method in the DFT framework within PBE potential using the WIEN2k code. The structural, electronic and optical properties of Cs_2NaBiI_6, $Cs_2NaBiBr_6$ and $Cs_2NaBiCl_6$ have been analysed. We have obtained the band gap of 2.0, 2.6 and 3.7 for Cs2NaBiI6, $Cs_2NaBiBr_6$ and $Cs_2NaBiCl_6$ respectively. Throughout the study, we have shown that the variation in the structure of double perovskite within Cs_2NaBiX_6(X=Cl, Br, I) that leads to the variation in band gap, density of states and in optical properties such as extinction coefficient, absorption spectra, optical reflectivity, dielectric coefficient, refractive index that shows the variety of this material for optoelectronic devices and other purposes.
Keywords: double perovskites; band gap, dielectric constant, optical conductivity
PACS: 73.21.−b; 73.30.+y; 73.40.Lq; 73.50.Gr

Nearly 85% of world's population are depending for energy on exhaustible fossil fuels that have deleterious outturn on human health & environmental consequences. Furthermore, this demand of energy will be double by 2050.The evolution of sustainable energy, like as hydrolic energy, wind energy and solar energy becomes an impending prerequisite [1]. Therefore, research to achieve high-efficient solar cells is currently very active. Perovskite becomes the most quickly developing solar cell because of their high power conversion efficiency and low cost. We all know that halide perovskite based solar cells are currently the fastest growing photovoltaic technology in terms of research and development. Firstly, reported hybrid organic inorganic halide perovskite $CH_3NH_3PbI_3$ as a light sensitizer in a dye-sensitize solar cell and demonstrated a power conversion efficiency of 3.8% [2].

Hybrid perovskites, such as $NH(CH_3)_3SnX_3$ (X = Cl, Br),[1] ABI_3 (A = CH_3NH_3, NH_2CHNH_2; B = Sn, Pb) [3] and $CH_3NH_3PbI_3$ [4] have been identified as potential candidates for fabricating high performance photovoltaic cells. Indeed, hybrid perovskites have considerable solar energy-conversion efficiency (greater than 19% [5]); however, they have some disadvantages, such as instability, a low resistance to moisture and heat when they are exposed for a long time to light and toxicity, which is caused by the presence of lead (Pb) [6,7]. Because of the mentioned diverse disadvantages of the hybrid perovskites, numerous researchers are working to identify an alternative to lead-halide perovskite semiconductors. Researchers have implemented a partial or full substitution of lead metal with tin or germanium in the perovskite structure. These modified materials, however, have resulted in inferior device performance due to the unstable +2 oxidation state of tin and germanium. Earlier predictions of new perovskite materials were based on the simple Goldschmidt tolerance factor to determine the stability of the structure. Recently, Travis et al. showed that the Goldschmidt tolerance factor fails to predict the stability of 32 known inorganic iodide perovskites. Researchers have been performed high throughput ab initio calculations on hypothetical three dimensional halide perovskites (ABX_3) obtained by substitution of lead with other divalent cations from the periodic table. The authors considered hundreds of material combinations and concluded that only Pb, Sn and Ge based perovskite show promising properties for optoelectronic devices. Attempts have also been made to find perovskite like structures via double perovskites, wherein two neighbouring divalent lead cations are replaced by monovalent and trivalent ones [8]. Double perovskites, a broad class of condensed materials has been started to investigated since 1960 [9, 10]. It was perhaps the most studied family of compound due to the flexibility of their structure, which permits novel device application originating from their low reactivity, magnetic and optical properties [11]. Double perovskites oxides, $AA'BB'O_6$, where A is alkaline-earth or rare-earth metal and B and B′ are transition metals, which are derived from simple ABO_3 perovskite, A-site atoms are alkaline earth metals such as Ba, Sr or a lanthanide and the B atoms are the transition metals. They constitute an important class of materials, characterized by structural distortion from the cubic, space group Fm3m (No. 225), structure. In this work, we contribute to the study of double perovskite Cs_2NaBiX_6 (X=Cl, Br, I) by performing a first principles study of their

† ***Cite as:*** S. Choudhary, S. Tomar, D. Kumar, S. Kumar, A.S. Verma, East. Eur. J. Phys. **3**, 74 (2021), https://doi.org/10.26565/2312-4334-2021-3-11

electronic and optical properties using the FPLAPW method in the DFT framework with PBE using the WIEN2k code [12]. We have performed the first principles calculations using the WIEN2k code based upon the framework of density functional theory (DFT) [13].

COMPUTATIONAL DETAILS

In this work, first principles calculations were executed within the framework of Kohn-Sham DFT to study the structural, electronic and optical properties of lead free halide double perovskite Cs_2NaBiX_6 (X = I, Br, Cl) by using Wien2k code [14, 15]. To optimize the lattice constant and ground state energy of lead free halide double perovskite the structural calculation was performed to properly relax the system in cubic phase using Wu-Cohen generalized gradient approximation (WC-GGA) giving optimized lattice constants. We employ a Perdew- Burke- Ernzerhof (PBE) generalized gradient approximation (GGA) exchange correlation functional [16]. For a well conversed SCF calculation, we used cut off energy -6.0 Ry, $R_{MT}\times K_{max}$ =7 and 125 k-points to create 5x5x5 k-mesh in the first Brillouin zone [17]. All present calculations were conducted using the full potential linearized augmented plane wave (FP-LAPW) method within the framework of density functional theory (DFT), as embodied in the WIEN2k code. The optical properties were determined for dense unit cell with 10000 k-mesh points. All the predictions are made using 0 K DFT relaxed structures and do not account for lattice expansion and temperature induced phase changes.

RESULTS AND DISCUSSIONS

Structural properties

The structural optimization based on Murnaghan's equation of state was performed to obtain the relax structure with minimum energy. Cs_2NaBiX_6 (X=Cl, Br, I) crystallizes in cubic phase (α=β=γ=90º) with space group. The exchange correlation effect is treated using Perdew-Burke Ernzerhof–Generalized-Gradient Approximation (PBE-GGA). By fitting the total energy versus the reduced and extended volume of the unit cell into third order Birch-Murnaghan's equation of states (EOS), the ground state structural properties such as equilibrium volume (V), Bulk modulus (B), pressure derivative of Bulk modulus (B′) and ground state energy (E_o) are determined[18,19].

$$E(V)=E_o+\frac{9V\,B}{16}\left\{\left[\left(\frac{V_o}{V}\right)^{2/3}-1\right]^3 B'+\left[\left(\frac{V_o}{V}\right)^{2/3}-1\right]^2 \text{x}\left[6-4\left(\frac{V_o}{V}\right)^{2/3}\right]\right\} \quad (1)$$

The energy vs. volume curve for Cs_2NaBiX_6 (X = Cl, Br, I) (obtained by geometry optimization) has been shown in figure (1) with displaying lattice parameters (a), equilibrium volume (V), bulk modulus (B), pressure derivative of bulk modulus (B′) for GGA-PBE potentials respectively. The value of internal parameter is decided by the convergence of total energy. The values of structural parameters are presented in table 1.

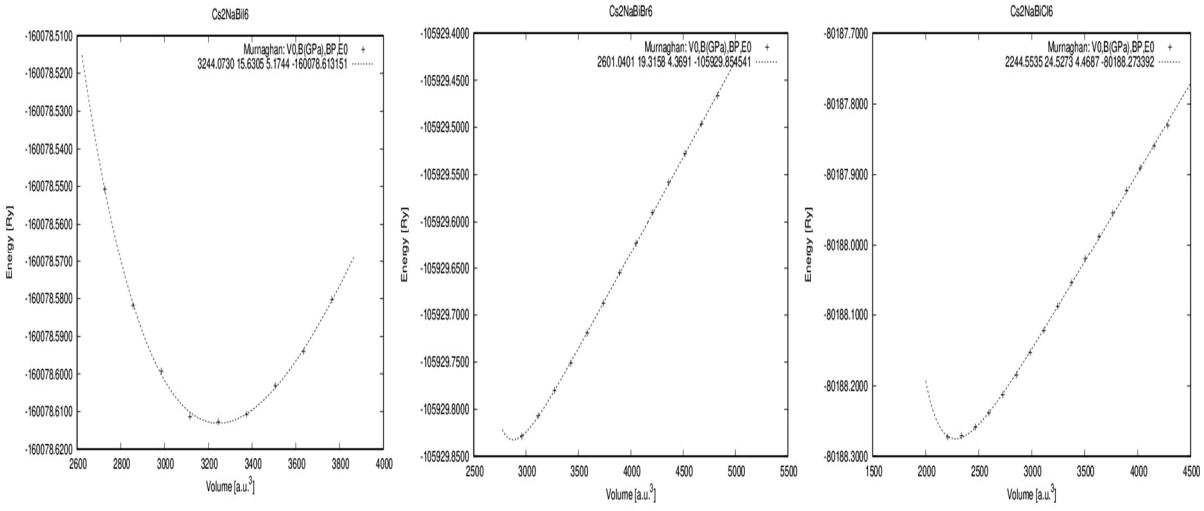

Figure 1. Volume optimization of Cs_2NaBiI_6, $Cs_2NaBiBr_6$ and $Cs_2NaBiCl_6$.

Table 1. Structural parameters of Cs_2NaBiX_6 (X = Cl, Br, I) perovskites.

Compounds	a_o(Å)	V(Å^3)	B (GPa)	B'
Cs_2NaBiI_6	21.75	3244.073	15.63	5.174
$Cs_2NaBiBr_6$	21.75	2601.040	19.31	4.369
$Cs_2NaBiCl_6$	21.72	2244.553	24.52	4.468

Electronic properties

The band structures of these compounds are presented in figure 2. From the band structure diagrams of Cs_2NaBiX_6 (X = Cl, Br, I) it is clear that there is a difference in band gap of three compounds and belongs to indirect band gap material,

because the maxima of valance band and minima of conduction band does not coincide at Γ-point. In this Ab- initio study, we have focused on lead free halide double perovskite Cs_2NaBiX_6 (X = Cl, Br, I). The most prominent difference among the studied compounds Cs_2NaBiI_6, $Cs_2NaBiBr_6$, and $Cs_2NaBiCl_6$ is their anions, which is responsible for the variation in the calculated band gap. From the graphs it has been observed the value of band gap is decreases rapidly from Cl to Br to I. It is due to the effect of anions. Anions play an important role and through the valence electron contribution they decrease the band gap. It's clear that the basic study of anions are plays an important role for the electronic and optical characteristic of photovoltaic devices. The calculated band gap for Cs_2NaBiX_6 (X = Cl, Br, I) along the high symmetric point of Brillion zone is 3.7, 2.6 and 2.0 eV respectively with the GGA–PBE exchange-correlation potential.

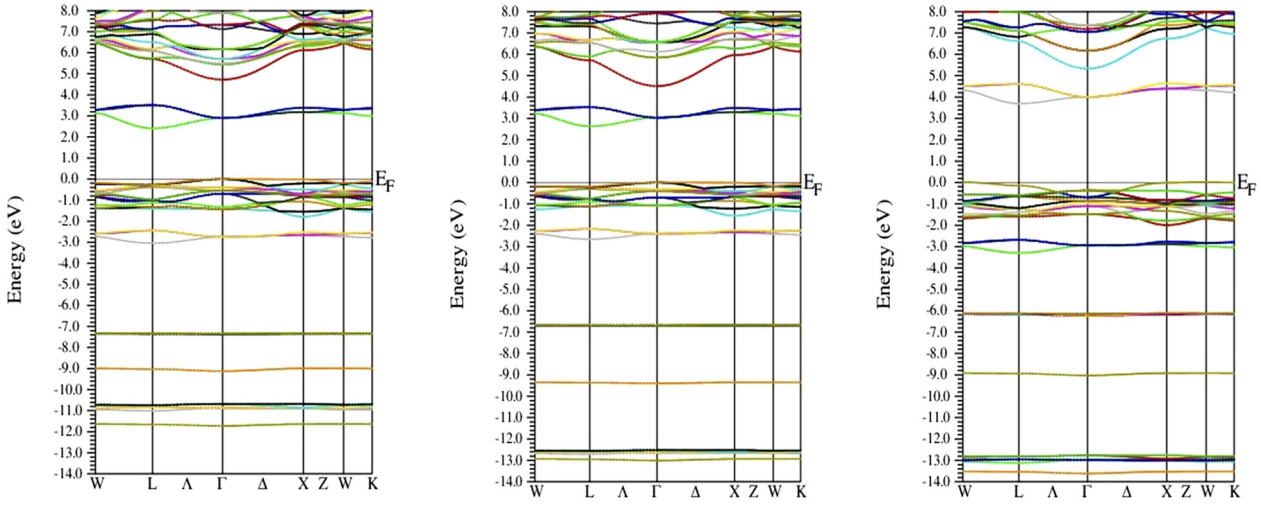

Figure 2. Band structure diagrams of Cs_2NaBiI_6, $Cs_2NaBiBr_6$ and $Cs_2NaBiCl_6$.

In diagram 3 the PDOS and TDOS of states of Cs_2NaBiX_6 (X = Cl, Br, I) has been presented. As we have seen in the plotted digram of PDOS for $Cs_2NaBiCl_6$ s and p orbital in upper valance band overlapped within the s and p of Na and Bi while s orbital of Cs and Na overlapped with s and p orbital of Cl. The lower valance band formed due to the overlapping of p orbital of Cs, Na, Bi and Cl. Similarly, in the case of $Cs_2NaBiBr_6$ and Cs_2NaBiI_6 the upper valance band mainly formed due to contribution of s orbital of Cs, Na, Bi and (X = Cl, Br, I) and lower valance band formed due to the p orbital overlapping in above compounds. From the above discussion, it can be said that the s orbital contribute more in all the case for formation of upper valance bands. Mutual hybridization of p orbital does not contribute that much to form upper valance band as compare to s orbital. We know that the position of the electron can be determined in all the compounds $Cs_2NaBiCl_6$, $Cs_2NaBiBr_6$ and Cs_2NaBiI_6 within upper valance band, lower valance band and conduction band. The total density of states (TDOS) for the lead free halide double perovskite $Cs_2NaBiCl_6$, $Cs_2NaBiBr_6$ and Cs_2NaBiI_6 represent the distribution of electrons in the energy spectrum. These figures describe the TDOS of Cs_2NaBiX_6 (X= Cl, Br, I) as well as for Na, Bi and (X=Cl, Br, I).

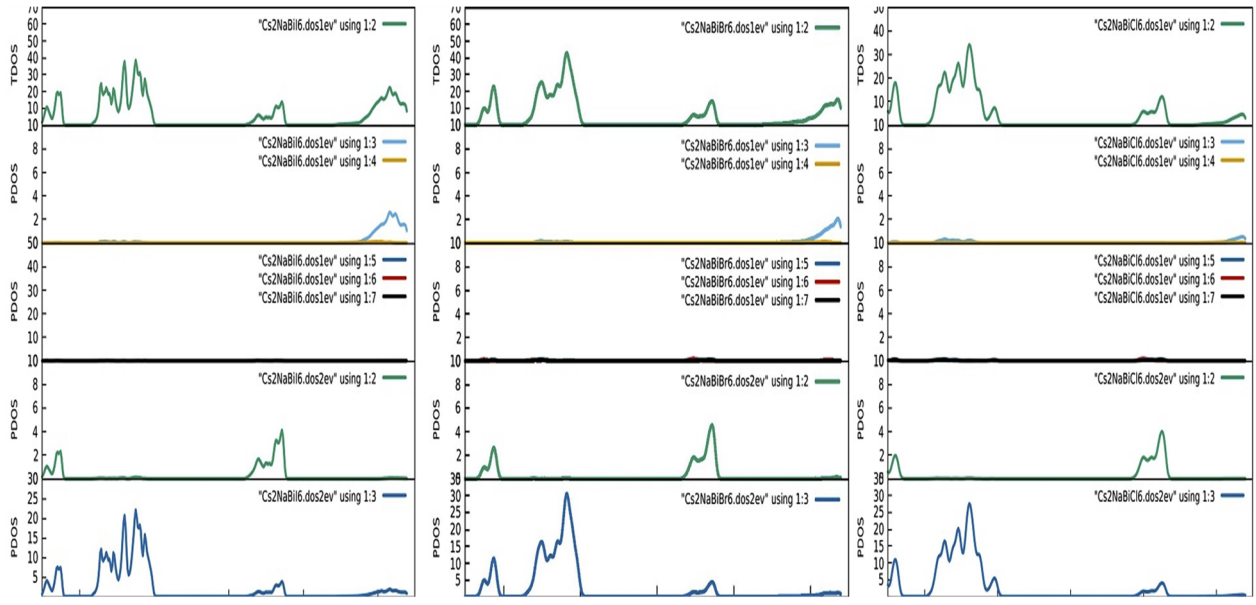

Figure 3. PDOS a nd TDOS diagrams of Cs_2NaBiI_6, $Cs_2NaBiBr_6$ and $Cs_2NaBiCl_6$

Optical properties

The dielectric properties are of great importance in giving insight into the fundamental physical properties and potential applications. The macroscopic optical response function of a compound is expressed by the dielectric function in the range of linear response. It is known that the dielectric function is mainly connected with the electronic response [20].

Basically, dielectric behavior of any compound is a quantity measuring the ability of a substance to store electrical energy in an electric field. The dielectric function known for describes the optical response of the medium at all photon energies [21] and gives a better understanding of electronic structure [22, 23]. The optical properties of Cs_2NaBiX_6 (X = Cl, Br, I) have been calculated from the complex dielectric function,

$$\varepsilon(\omega) = \varepsilon_1(\omega) + \varepsilon_2(\omega)$$

The imaginary part $\varepsilon_2(\omega)$ was calculated from momentum matrix elements between the occupied and unoccupied wave functions within the selection rules. The imaginary part $\varepsilon_2(\omega)$ of dielectric function can be express energy loss or describe the density of Plasmon excitation in a system. The variation of real part $\varepsilon_1(\omega)$ and imaginary part $\varepsilon_2(\omega)$ of dielectric function with respect to photon energy are shown in figure 4. This can be observed from the results that from IR to visible to UV region (0 – 4.31 eV) , Cs_2NaBiX_6 (Cl, Br, I) shown higher dielectric constant ranges . In case of $Cs_2NaBiCl_6$ it reaches its first maximum value 5.29 at 4.38 eV. Similarly in $Cs_2NaBiBr_6$ and Cs_2NaBiI_6 shown higher peaks 6.47 at 2.9eV and 7.28 at 2.8 eV respectively corresponding to first and second inter band transition at R and M symmetry points of Brilliouin zone for Cs_2NaBiX_6 (Cl, Br, I) along with $\varepsilon_1(\omega)$. Figure 4 shows the frequency dependent absorptive part $\varepsilon_2(\omega)$ of dielectric function $\varepsilon(\omega)$, the maximum absorption behaviour of these materials represented by the value of real part of dielectric constant as well as the value of $\varepsilon_2(\omega)$ start increasing sharply with the incident electromagnetic radiation. The threshold energy points occur for Cs_2NaBiX_6 (Cl, Br, I) at 2.8 eV, 2.24 eV and 2.18 eV respectively. After these threshold energy points many peaks can be seen that corresponds to the inter band transition for valence band to transition band. We can directly calculate the optical quantities like optical conductivity, absorption co efficient, refractive index, reflectivity etc. by using the real and imaginary part of dielectric function by the relation described in the reference [24].

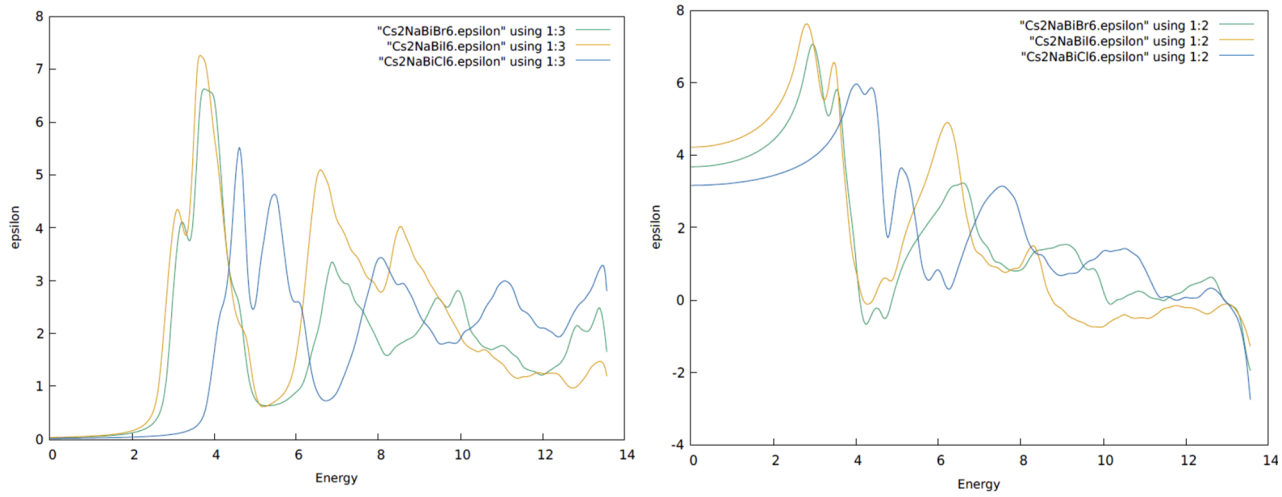

Figure 4. The plotted curve between photon energy and dielectric parameters imaginary epsilon ($\varepsilon_2(\omega)$) and real epsilon ($\varepsilon_1(\omega)$)

The absorption coefficient determines how far into a material light of a particular wavelength can penetrate before it get absorbed; it depends on the material and also on the wavelength of light which is being absorbed. Figure 5 gives a wide interpretation of absorption spectra Cs_2NaBiX_6 (X = Cl, Br, I) and its clear from the graph that the stronger absorption is seen from visible region to the commence of UV region i.e., in case of $Cs_2NaBiCl_6$ it ranges from 2.8-4.9eV, for $Cs_2NaBiBr_6$ it ranges from 2.2- 4.1eV and for Cs_2NaBiI_6 it ranges from 2.1- 4.2eV respectively. Instead of photon absorption there are several numbers of ways of exciting electrons in a compound. First is subjected to optical spectra is the excitation of electrons by other electrons that is done by shining a beam of mono-energetic electrons at a sample and analyzing the energy of the transmitted or reflected beam. It is found that the incident electrons loss energy in discrete amounts. The loss spectrum arises both from the excitation of single electros in solid, just as in the case of photon absorption and also from the excitation of collective oscillations called Plasmon's. In case of inter-band transitions, which consist most of the Plasmon excitations, the scattering probability of volume losses is directly related to the energy loss function L(ω) [19]. The energy loss function L(ω) is also displayed in figure 5. This function plays an important role describing the energy loss of a fast electron traversing in a material. The peaks in L(ω) spectra represent the characteristic associated with the plasma resonance. The resonant energy loss from the help of the graph can be seen at 6.24eV, 4.52eV and 4.4eV in $Cs_2NaBiCl_6$, $Cs_2NaBiBr_6$ and Cs_2NaBiI_6 respectively.

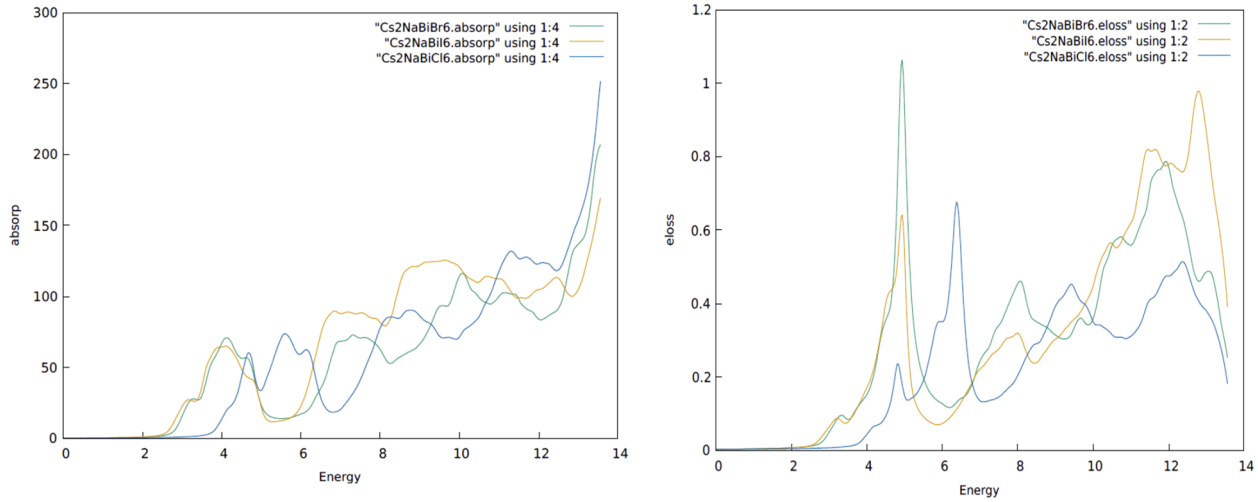

Figure 5. Absorption spectra and Energy loss function L(ω) of Cs_2NaBiX_6 (X =Cl, Br, I).

Refractive index of any material is a dimensionless number that describes how fast light travels through the materials. The refractive index and extinction coefficient are displayed in figure 6. We have observed the optically isotropic nature of this compound in the lower energy range. For lower energies the refractive index value is almost constant and as the energy increases it attains a maximum value and exhibits decreasing tendency for higher energy values. The static refractive index n(0) is found to have the value 1.78, 1.90, and 2.1 in cases of $Cs_2NaBiCl_6$, $Cs_2NaBiBr_6$ and Cs_2NaBiI_6 respectively. It increases with energy in the transparent region reaching a peak in the ultraviolet range at 4.6 eV for $Cs_2NaBiCl_6$, and in visible region at 3.0 eV and 2.8 eV for $Cs_2NaBiBr_6$ and Cs_2NaBiI_6 respectively. The refractive index is greater than one because as photons enter a material they are slowed down by the interaction with electrons [20]. The more photons are slowed down while travelling through a material, the greater the material's refractive index. Generally, any mechanism that increases electron density in a material also increases refractive index. However, refractive index is also closely related to bonding. In general, ionic compounds are having lower values of refractive index than covalent ones. In covalent bonding more electrons are being shared by the ions than in ionic bonding and hence more electrons are distributed through the structure and interact with the incident photons to slow down.

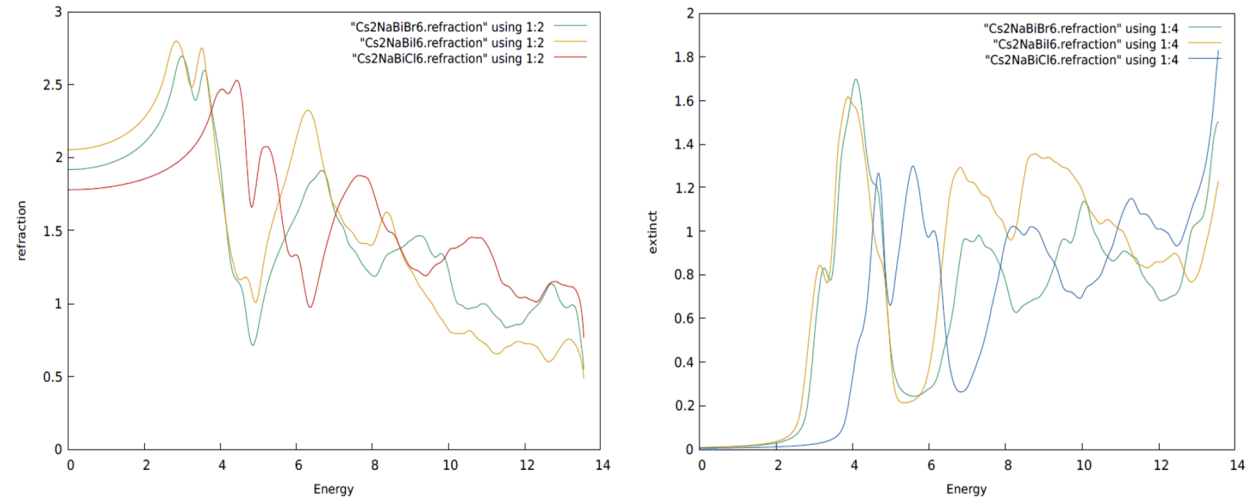

Figure 6. Refraction coefficient n(ω) and Extinction coefficient K(ω) of Cs_2NaBiX_6 (M = Cl, Br, I).

As extinction coefficient (K) is a measure of light lost due to scattering and absorption per unit volume, hence, high values of K in lower wavelength range show that these films are opaque in this range. Extinction coefficient reached its highest peaks at 4.8 eV, 4.0 eV and 3.8 eV for $Cs_2NaBiCl_6$, $Cs_2NaBiBr_6$ and Cs_2NaBiI_6 respectively. As we have observed the extinction coefficient and imaginary part of dielectric parameters they show a similar trend. $Cs_2NaBiCl_6$ and $Cs_2NaBiBr_6$ shows highest peaks in UV region and Cs_2NaBiI_6 shows a highest peak in UV region and a small peak in visible region as we have seen from the plotted figure 7. Reflectivity is an optical property of material, which describes how much light is reflected from the material in relation to an amount of light incident on the material. The reflectance occurs always on the surface of the material, for the light diffusing materials also in the volume of the materials. As shown in figure 7 the reflective coefficient as a function of photon energy. Reflective spectra of $Cs_2NaBiCl_6$ shows promise in UV region ranges between 4.0eV to 6.0eV. From these figures of $Cs_2NaBiCl_6$, it is clear that these materials show good reflectivity in UV region so that it can be a promising material to use as a UV detector.

As in the case of $Cs_2NaBiCl_6$, the reflective spectra of $Cs_2NaBiBr_6$ show a good agreement in between visible to UV range in the spectra. The reflectivity of this material ranges from 3.0eV to 4.8eV.This material is will be useful as an optoelectronic device as well as in UV generators. Cs_2NaBiI_6 shows good spectra in visible to UV range. It ranges from 2.8 eV to 4.1 eV. The optical conductivity is shown in figure 7. In case of $Cs_2NaBiCl_6$ it ranges from 3.9 eV to 13.5 eV, similarly in $Cs_2NaBiBr_6$ it ranges from 2.8 eV to 13.3 eV and in case of Cs_2NaBiI_6 it ranges in between 2.3 to 8.3 eV.

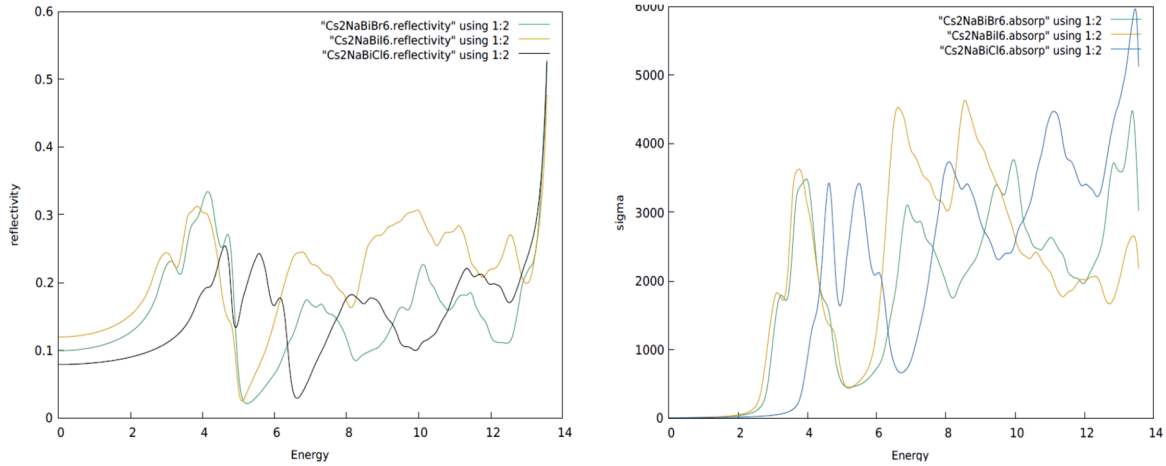

Figure 7. Optical Reflectivity R(ω) and (I) Optical conductivity σ(ω) of Cs_2NaBiX_6 (X = Cl, Br, I).

SUMMARY AND CONCLUSIONS:

In this work, we have studied the structural, electronic, and optical properties of the lead free halide double perovskite $Cs_2NaBiCl_6$, $Cs_2NaBiBr_6$ and Cs_2NaBiI_6 using the FP-LAPW method within the local density approximation (LDA), generalized gradient approximation (GGA) in the framework of density functional theory. The optical properties such as dielectric function, reflectivity, absorption coefficient, optical conductivity, refractive index, and extinction coefficient and energy loss are studied. These calculations revels that $Cs_2NaBiCl_6$ and $Cs_2NaBiBr_6$ shows better behavior in UV range and can be used as UV generators while $Cs_2NaBiBr_6$ and Cs_2NaBiI_6 shows a good band gaps in visible region and can be used in lead free, non-toxic optoelectronic devices. However, we expect that this present study will motivate to experimental investigation on electronic and optical properties of lead free halide double perovskite.

ORCID IDs

Shaily Choudhary, https://orcid.org/0000-0003-4211-0921; **Shalini Tomar**, https://orcid.org/0000-0001-7385-3061
Depak Kumar, https://orcid.org/0000-0002-2958-8309; **Sudesh Kumar**, https://orcid.org/0000-0002-7507-4712
Ajay Singh Verma, https://orcid.org/0000-0001-8223-7658

REFERENCES

[1] H. Tang, S. He, and C. Peng, Nanoscale Research Letters, **12**, 410 (2017), https://doi.org/10.1186/s11671-017-2187-5
[2] F. Giustino, and H.J. Snaith, ACS Energy Letters, **1**, 1233 (2016), https://doi.org/10.1021/acsenergylett.6b00499
[3] Y. Dang, C. Zhong, G. Zhang, D. Ju, L. Wang, S. Xia, H. Xia, and X. Tao, Chem. Mater. **28**, 6968 (2016), https://doi.org/10.1021/acs.chemmater.6b02653
[4] C. Lee, J. Hong, A. Stroppa, M.H. Whangbo, and J.H. Shim, RSC Adv. **5**, 78701 (2015), https://doi.org/10.1039/C5RA12536G
[5] T. Zhao, W. Shi, J. Xi, D. Wang, and Z. Shuai, Sci. Rep. **7**, 19968 (2016), https://doi.org/10.1038/srep19968
[6] H.S. Jung, and N.G. Park, Small, **11**, 10 (2015), https://doi.org/10.1002/smll.201402767
[7] A.H. Slavney, R.W. Smaha, I.C. Smith, A. Jaffe, D. Umeyama, and H.I. Karunadasa, Inorg. Chem. **56**, 46 (2017), https://doi.org/10.1021/acs.inorgchem.6b01336
[8] F. Giustino, and H.J. Snaith, ACS Energy Lett. **1**, 1233 (2016), https://doi.org/10.1021/acsenergylett.6b00499
[9] J. Cheng, and Z.Q. Yang, Physica Status Solidi B, **243**, 1151 (2006), https://doi.org/10.1002/pssb.200541381
[10] H. Wu, Phys. Rev. B, **64**, 125126 (2001), https://doi.org/10.1103/PhysRevB.64.125126
[11] Y. Shimakawa, M. Azuma, and N. Ichikawa, Materials, **4**, 153 (2011), https://doi.org/10.3390/ma4010153
[12] P. Blaha, G.K.H. Madsen, D. Kvasnicka, and J. Luitz, *WIEN2K, an augmented plane wave plus local orbitals program for calculating crystal properties* (Vienna, Austria) 2008.
[13] P. Hohenberg, and W. Kohn, Phys. Rev. **136**, B864 (1964), https://doi.org/10.1103/PhysRev.136.B864
[14] W. Kohn, and L.J. Sham, Phys. Rev. **140**, A1133 (1965), https://doi.org/10.1103/PhysRev.140.A1133
[15] J.P. Perdew, A. Ruzsinszky, G.I. Csonka, O.A. Vydrov, G.E. Scuseria, L.A. Constantin, X. Zhou, and K. Burke, Phys. Rev. Lett. **100**, 136406 (2008), https://doi.org/10.1103/PhysRevLett.100.136406
[16] J.P. Perdew, K. Burke, and M. Ernzerhof, Phys. Rev. Lett. **77**, 3865 (1996), https://doi.org/10.1103/PhysRevLett.77.3865
[17] H.J. Monkhorst, and J.D. Pack, Phys. Rev. B, **13**, 5188 (1976), https://doi.org/10.1103/PhysRevB.13.5188
[18] F. Birch, Physical Review, **71**, 809 (1947), https://doi.org/10.1103/PhysRev.71.809
[19] F.D. Murnaghan, Proc. Natl. Acad. Sci. USA, **30**, 244 (1994), https://dx.doi.org/10.1073%2Fpnas.30.9.244

[20] E.E. Eyi, and S. Cabuk, Philosophical Magazine, **90**, 2965 (2010), https://doi.org/10.1080/14786431003752159
[21] K.E. Babu, N. Murali, K.V. Babu, P.T. Shibeshi, and V. Veeraiah, Acta Physica Polonica A, **125**, 1179 (2014), http://dx.doi.org/10.12693/APhysPolA.125.1179
[22] M.L. Ali, and M.Z. Rahaman, Int. J. Mater. Sci. Appl. **5**, (2016) 202-206, https://doi.org/10.11648/j.ijmsa.20160505.14
[23] S. Choudhary, A. Shukla J. Chaudhary, and A.S. Verma, Int. J. Energy Res. **44**, 11614 (2020), https://doi.org/10.1002/er.5786
[24] R. Gautam, P. Singh, S. Sharma, S. Kumari, and A.S. Verma, Superlattice Microst. **85**, 859 (2015), https://doi.org/10.1016/j.spmi.2015.07.014

ДОСЛІДЖЕННЯ БЕЗСВИНЦЕВИХ ГАЛІДІВ У ПОДВІЙНИХ ПЕРОВСКІТАХ НА ОСНОВІ НАТРІЮ Cs2NaBiX6 (X = Cl, Br, I): НЕЕМПЕРІЧНЕ (AB INITIO) ДОСЛІДЖЕННЯ

Шайлі Чоудхарі[a], Шаліні Томар[a], Депак Кумар[a], Судеш Кумар[c], Аджай Сінгх Верма[d]
[a]*Фізичний факультет, Банастхалі Відьяпітх, Банастхалі, Раджастан, 304022, India*
[b]*Department of Chemical Engineering, Банастхалі Відьяпітх, Банастхалі 304022, Індія*
[c]*Фізичний факультет, Банастхалі Відьяпітх, Банастхалі, Раджастан, 304022, Індія*
[d]*Факультет природничих та прикладних наук, університет Глокал, Сахаранпур, 247232, Індія*

Незважаючи на значні переваги перовскітних оптоелектронних пристроїв на основі свинцю, їх нестабільний характер та токсичність все ще є перешкодою для практичного застосування. Подвійний перовскіт став кандидатом для застосування в оптоелектроніці та фотоелектричній техниці через його нетоксичний характер та стабільність у повітрі. Ми представили неемперічне (ab-initio) дослідження безсвинцевих галогенідних подвійних перовскітів Cs_2NaBiX_6(X=Cl, Br, I). Розрахунок проводиться за допомогою методу FP-LAPW в рамках DFT в межах потенціалу PBE з використанням коду WIEN2k. Були проаналізовані структурні, електронні та оптичні властивості Cs_2NaBiI_6, $Cs_2NaBiBr_6$ та $Cs_2NaBiCl_6$. Ми отримали ширину енергетичної щілини 2,0, 2,6 та 3,7 для Cs_2NaBiI_6, $Cs_2NaBiBr_6$ та $Cs_2NaBiCl_6$ відповідно. Протягом усього дослідження ми показали, що зміна структури подвійного перовскіту в межах Cs_2NaBiX_6 (X = Cl, Br, I), що призводить до зміни ширини енергетичної щілини, щільності станів та оптичних властивостей, таких як коефіцієнт згасання, спектри поглинання, оптична відбивна здатність, діелектричний коефіцієнт, показник заломлення свідчить про різноманітність цього матеріалу для оптоелектронних пристроїв та інших цілей.

Ключові слова: подвійні перовскіти, ширина енергетичної щілини, діелектрична проникність, оптична провідність